# Influence of soil structure interaction on the 4th story building

*Alex* Kurniawandy[1*], *Cindy* Dayu Tiara[1], *Riza* Aryanti[2], and *Muhammad* Aminsyah[2]

[1]Civil Engineering Department, Faculty of Engineering, Riau University, Pekanbaru, Riau, Indonesia
[2]Civil Engineering Department, Faculty of Engineering, Universitas Andalas, Padang, West Sumatra, Indonesia

**Abstract.** Design structure generally is carried out using fixed-based restraints, which assume soil is infinitely rigid. The soil has a certain rigidity and can deform a structure commonly called soil structure interaction (SSI). However, practitioners rarely consider interaction between soil and structural systems because of their high complexity and long computing time. The SSI reviews need to be carried out to obtain a more accurate analysis according to original conditions in the soil. The study aims to identify structural behavior with consideration of SSI in a case study of the 4th-story building in Pekanbaru. Structural analysis is done linearly using response spectrum analysis and nonlinear pushover analysis. Modeling was made into two types: model 1 using fixed base and model 2 using spring located on the points along the pile foundation as a representation of SSI. The analysis results show the natural period increases by 20% in the X direction and 18% in Y. The base shear decreases by 18% in the X direction and 16% in Y. The maximum displacement increases by 29% in the X direction and 24% in Y. Nonlinear pushover analysis results in an increase in the performance point value of structure with SSI modeling.

## 1 Introduction

Modeling structures using pinch supports assumes that the subgrade is rigid so that when the structural system is given an earthquake load, only the upper structure deforms while the soil does not move. This assumption is not in accordance with field conditions where, during an earthquake, the soil will experience movement. The process by which soil response and structural motion influence each other is called soil structure interaction [1-3].

Generally, structural analysis performed by practitioners rarely considers the interaction between soil and structure. However, soil-structure interaction has a prominent influence on heavy construction and construction built on soft soil. Therefore, it is necessary to review aspects of soil-structure interaction to obtain data closer to the field's original conditions.

Investigating the magnitude of the effect of soil-structure interaction (SSI) can be done by analyzing the behavior of the structure through linear analysis that occurs when the building is in elastic condition. The effect of soil-structure interaction (SSI) is closely related to dynamic loads. Therefore, linear analysis is performed with dynamic analysis using earthquake response spectrum data, which is considered more efficient in the computational process but can still provide a global picture and sufficient information about the structure's response to dynamic loads.

In addition, it is also necessary to consider the performance of structures involving SSIs to see if there is a change in structural performance when SSI are considered in the analysis. Structural performance analysis can be performed using advanced nonlinear pushover analysis, which is commonly used. This nonlinear pushover analysis is carried out to analyze the inelastic behavior of the structure against various earthquake intensities applied to the structure so that the performance of the structure in critical conditions can be known [4].

Therefore, the author will conduct a structural analysis by considering soil-structure interaction (SSI) to identify how much influence SSI has on structural response and structural performance. This research will discuss the influence of SSI on the existing 4th-story building in Pekanbaru City, Riau Province. This building uses reinforced concrete as its main material. The structural analysis was conducted using a linear dynamic analysis approach with earthquake response spectrum data and nonlinear pushover analysis. This research output compares base shear force, vibration period, displacement, and structural performance in structural analysis with and without SSI consideration.

## 2 Methodology

This research uses an existing structure as a case study with a structural system in the form of a moment-bearing frame system. This building is located in Pekanbaru City and is categorized as having medium soil (SD). Structural element data, loading data, and soil data are based on the detailed engineering design document of the building used as the object.

* Corresponding author: alexkurniawandy@eng.unri.ac.id

Soil structure interaction (SSI) modeling is performed using the indirect deformable piles interactive spings method by modeling the upper structure and lower structure in pile foundations into a single substructure. The soil is then modeled as a spring by inputting dynamic stiffness values that relate dynamic loads to displacements at several points of contact between the soil and foundation.

The soil spring stiffness in pile foundations consists of three types: the vertical direction spring at the base of the pile (end bearing), the horizontal direction lateral spring along the pile, and the vertical skin friction resistance spring (skin friction). An illustration the three types of springs can be seen in Fig. 1 below.

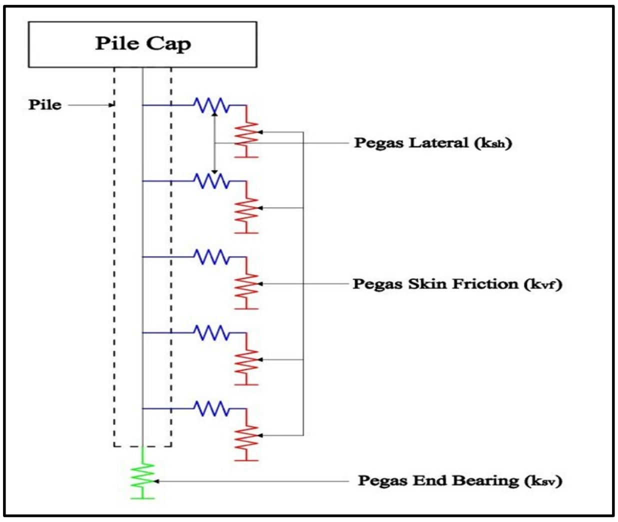


**Fig 1.** Illustration of soil-structure interaction in pile foundations

The soil spring stiffness in the horizontal and vertical directions can be calculated using the subgrade reaction modulus parameter ($K_s$) obtained through the Equation. (1) as follows [4]:

$$K_s = \frac{0.65}{D} \times \sqrt[12]{\frac{E_s D^4}{E_p I_p}} \times \frac{E_s}{1-\mu_s^{\,2}} \tag{1}$$

In which:
$K_s$ = modulus of subgrade reaction (kN/m$^3$)
$E_s$ = modulus of soil elasticity (kN/m$^2$)
$E_p$ = modulus of elasticity of the foundation (kN/m$^2$)
$I_p$ = foundation cross-section inertia (kg/cm$^2$)
$\mu_s$ = soil Poisson's ratio
$D$ = pole diameter or pole side dimension (m)

The vertical direction spring stiffness at the base of the pile ($K_{sv}$) can be calculated using the Equation (2) below:

$$K_{sv} = K_s \times A_p \tag{2}$$

In which:
$K_{sv}$ = end bearing spring stiffness (kN/m$^2$)
$A_p$ = cross-sectional area of the pile (m$^2$)

The horizontal direction spring stiffness along the pile ($K_{sh}$) can be calculated using the Equation (3) below:

$$K_{sh} = K_s \times D \times L \tag{3}$$

In which:
$K_{sh}$ = horizontal direction spring stiffness (kN/m$^2$)
$L$ = length of pile foundation (m)

The stiffness of the vertical skin friction resistance spring ($K_{vf}$) can be calculated using the Equation (4) below:

$$K_{vf} = 1.8 \times E_s \times \eta \times \lambda^{(0.5-\frac{\lambda}{\eta})} \times \alpha \tag{4}$$

In which:
$K_{vf}$ = skin friction spring stiffness (kN/m$^2$)
$\eta$ = pile ratio
λ = pile-soil stiffness ratio
α = vertical spring stiffness effect along the pile length

The values of pile ratio (η) and pile-soil stiffness ratio (λ) can be calculated using the Equations (5) and (6) below:

$$\eta = \frac{L}{D} \tag{5}$$

$$\lambda = \frac{E_p}{E_s} \tag{6}$$

The α value is an expression used to distribute the effect of soil vertical stiffness along the pile. The value of α = 1.00 is used for the spring positioned at the base of the pile. While the value of α used for the spring along the pile can be calculated using the Equation (7) below:

$$\alpha = \frac{Z \times \Delta_z}{L^2} \tag{7}$$

In which:
$Z$ = depth of spring placement point (m)
$\Delta_z$ = distance between springs (m)

The spring stiffness values were calculated based on soil investigation by using Cone Penetration Test (CPT) at the construction site. Equations (1) to (7) are carried out to determine the stiffness and result of the calculation presented in Table 1 below.

**Table 1.** Calculation results of ground spring stiffness

| Soil Depth (m) | $K_{sh}$ (kN/m) | $K_{vf}$ (kN/m/m) | $K_{sv}$ (kN/m) |
|---|---|---|---|
| 1 | 12,124.81 | 0 | - |
| 2 | 26,308.18 | 0 | - |
| 3 | 62,249.65 | 0 | - |
| 4 | 154,325.83 | 0 | - |
| 5 | 327,005.03 | 0 | - |
| 6 | 291,731.83 | 0 | - |
| 7 | 380,461.25 | 0 | - |
| 8 | 398,413.57 | 0 | - |
| 9 | 160,706.13 | 0 | - |
| 10 | 75,843.19 | 0 | - |
| 11 | 452,636.27 | 0 | - |
| 12 | 340,524.42 | 0 | - |
| 13 | 398,413.57 | 0 | - |
| 14 | 264,384.39 | 0 | - |
| 15 | 371,370.33 | 0 | - |
| 16 | 692,899.53 | 0 | 12,991.87 |

## 3 Numerical model

This study uses two types of structural models, namely model 1 in the form of a top structure with a pinch support and model 2 in the form of a top structure and bottom structure modeled as a whole with a spring support placed at the nodal along the pile foundation as a representation of SSI. Model 1 (fixed base) and model 2 (SSI) used in this study are presented in Figs. 2 and 3.

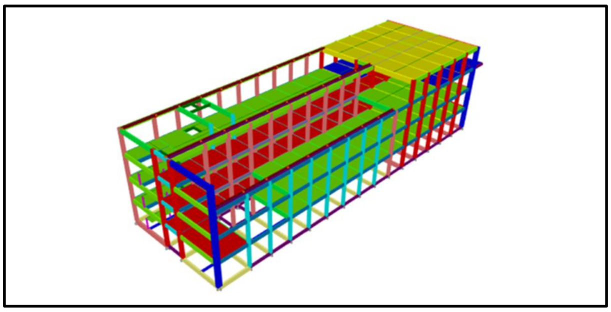

**Fig 2.** Model 1 fixed base

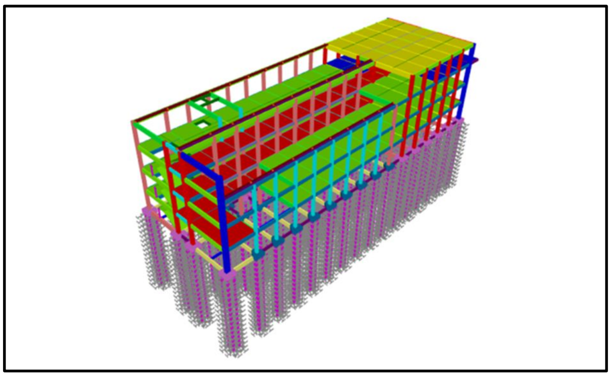

**Fig 3.** Model 2 soil structure interaction (SSI)

The structural analysis is carried out with a linear dynamic analysis approach with earthquake response spectrum data and further analysis in the form of nonlinear static analysis (pushover analysis) [5-7]. The plan response spectrum used is based on the Indonesian National Standard SNI 1726: 2019 based on the location of the building [8].

The building is located in Pekanbaru, and the design earthquake parameters include a short-period acceleration ($S_s$) of 0.453 g, and a 1-s period acceleration ($S_1$) of 0.281 g. The response spectrum graph is presented in Fig. 4 below.

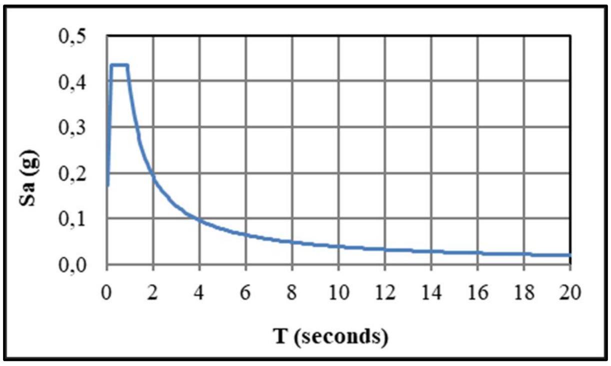


**Fig 4.** Design response spectral at the location of the existing building

Further analysis in the form of nonlinear pushover analysis was conducted based on ASCE 41 [9]. The nonlinear pushover analysis output in the form of a capacity curve is a graph of the relationship between the shear force applied to the structure and increased periodically with the displacement that occurs at the review point due to the application of the previous load.

## 4 Results and discussion

The results of the comparison of the two structural models show that the consideration of SSI in the existing structure produces an increase in the natural period of the structure, as can be seen in Table 2.

**Table 2.** Natural period of the structure

| Structure Model | Period (seconds) | |
|---|---|---|
| | X | Y |
| Model 1 (Fixed Base) | 0.98 | 0.90 |
| Model 2 (Soil-Structure Interaction) | 1.18 | 1.06 |

The results of the comparison of the natural periods of the two models are presented in Fig. 5 below.

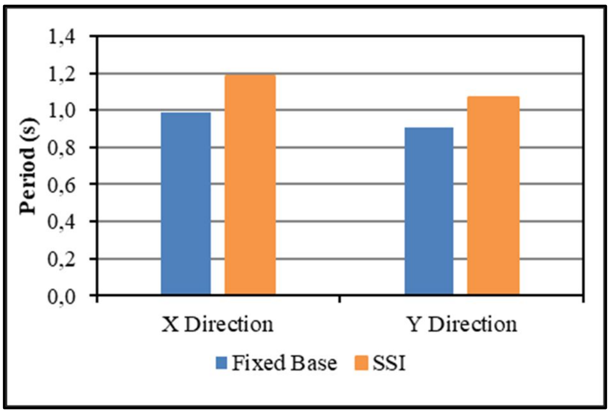


**Fig 5.** Comparison of natural period of structures

### 4.1 Shear force

The comparison of the two structural models shows that the consideration of SSI in the existing structure resulted in an increase in the base shear force of the structure, which can be seen in Table 3.

**Table 3.** Shear force of structure

| Structure Model | Shear Force (kN) | |
|---|---|---|
| | X | Y |
| Model 1 (Fixed Base) | 2,990.98 | 3,258.97 |
| Model 2 (Soil-Structure Interaction) | 2,466.50 | 2,740.16 |

The results of the comparison of the natural periods of the two models are presented in Fig. 5 above and Fig. 6 below.

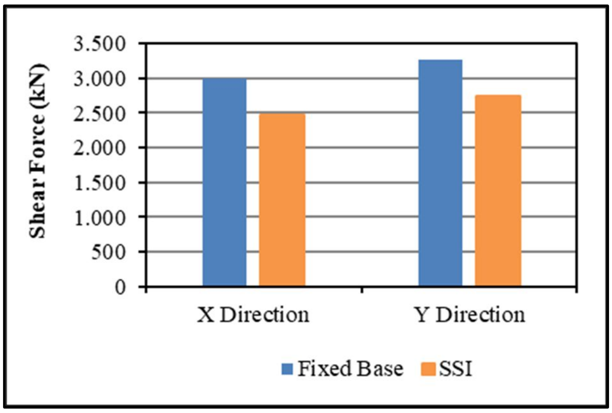


**Fig 6.** Comparison of structure base shear force

The results of the comparison of the two structural models show that the consideration of SSI in the existing structure results in changes in the distribution of shear forces received by each floor of the structure, which can be seen in Tables 5 and 6.

**Table 4.** Shear force distribution for fixed-based structure

| Story | Elevation (m) | Position | Shear Force (kN) | |
|---|---|---|---|---|
| | | | X dir. | Y dir. |
| 4 | 15.95 | Top | 751.35 | 810.58 |
| | | Bottom | 751.35 | 810.58 |
| 3 | 11.95 | Top | 1,790.35 | 1,954.51 |
| | | Bottom | 1,802.05 | 1,967.72 |
| 2 | 7.95 | Top | 2,579.53 | 2,825.12 |
| | | Bottom | 2,587.31 | 2,833.21 |
| 1 | 3.95 | Top | 2,987.90 | 3,256.41 |
| | | Bottom | 2,990.98 | 3,258.97 |
| Base | 0.0 | Top | 0 | 0 |
| | | Bottom | 0 | 0 |

As shown in Tables 4 and 5, the shear force distribution in the SSI model is higher than that in the fixed-base model.

**Table 5.** Shear force distribution for SSI structure

| Story | Elevation (m) | Position | Shear Force (kN) | |
|---|---|---|---|---|
| | | | X dir. | Y dir. |
| 4 | 15.95 | Top | 573.89 | 624.07 |
| | | Bottom | 573.89 | 624.07 |
| 3 | 11.95 | Top | 1,386.86 | 1,535.18 |
| | | Bottom | 1,396.26 | 1,546.06 |
| 2 | 7.95 | Top | 2,032.27 | 2,277.63 |
| | | Bottom | 2,039.14 | 2,285.15 |
| 1 | 3.95 | Top | 2,462.58 | 2,736.71 |
| | | Bottom | 2,466.51 | 2,740.16 |
| Base | 0.0 | Top | 2,488.27 | 2,763.71 |
| | | Bottom | 0.00 | 0.00 |

The results of the comparison of shear force distribution for each floor of the structure are presented in Figs. 7 and 8 below.

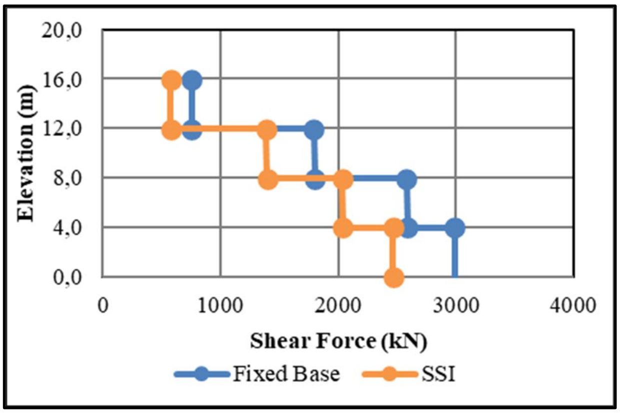


**Fig 7.** Shear force distribution in X-direction

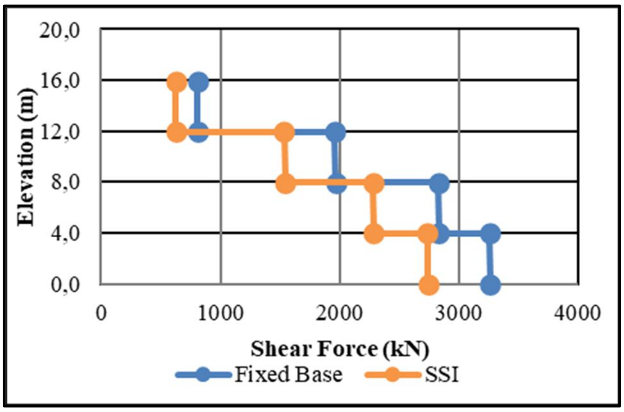


**Fig 8.** Shear force distribution in Y-direction

## 4.2 Maximum displacement

The results of the comparison of the two structural models show that the consideration of SSI in the existing structure results in an increase in the maximum displacement of each floor of the structure, which can be seen in Tables 6 and 7 below.

**Table 6.** Maximum displacement of model 1

| Story | Elevation (m) | Displacement (mm) | |
|---|---|---|---|
| | | X dir. | Y dir. |
| 4 | 15.95 | 25.96 | 33.32 |
| 3 | 11.95 | 20.52 | 27.89 |
| 2 | 7.95 | 14.13 | 17.24 |
| 1 | 3.95 | 6.05 | 7.27 |
| Base | 0.0 | 0.00 | 0.00 |

**Table 7.** Maximum displacement of model 2

| Story | Elevation (m) | Displacement (mm) | |
|---|---|---|---|
| | | X dir. | Y dir. |
| 4 | 15.95 | 29.85 | 37.37 |
| 3 | 11.95 | 25.21 | 31.96 |
| 2 | 7.95 | 18.89 | 22.21 |
| 1 | 3.95 | 10.57 | 12.11 |
| Base | 0.0. | 1.99 | 2.17 |

The results of the displacement comparison for each floor of the structure are presented in Figs. 9 and 10 below.

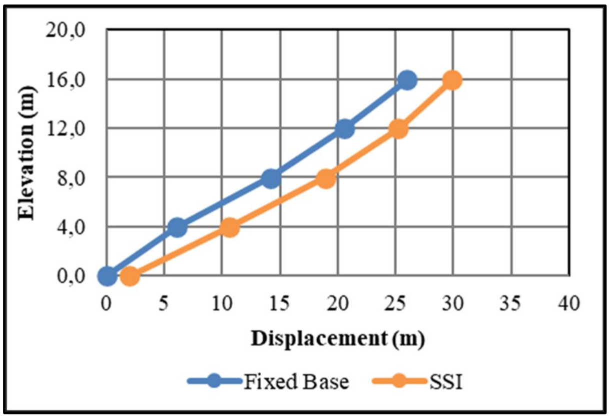


**Fig 9.** Maximum displacement in x-direction

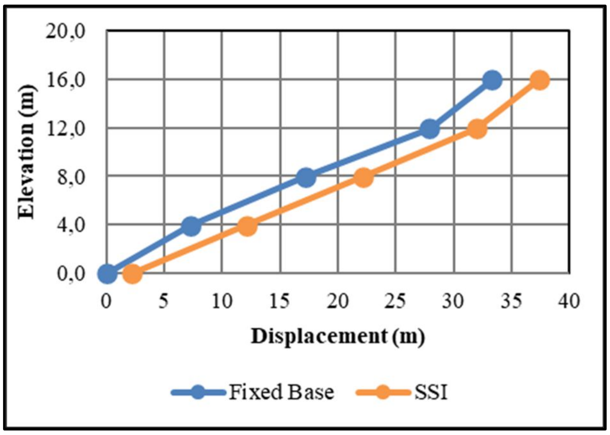


**Fig 10.** Maximum displacement in y-direction

It can be seen from the above figure that for the SSI model there is a shift in the restraint base of the structure. Then, the displacement of the SSI model is larger than that of the fixed-base model. The trend or shape of the displacement of each floor is almost identical for both models.

### 4.3 Story drift

The results of the comparison of the two structural models shows that the consideration of SSI in the existing structure results in changes in story drift, which can be seen from Tables 8-11.

**Table 8.** Story drift fixed base structure in x-direction

| Story | Floor Height h | Displ $\delta_X$ | Elastic Drift $\Delta_{elastic}$ | Inelastic Drift $\Delta_{inelastic}$ | Drift Ratio X |
|---|---|---|---|---|---|
| | (mm) | (mm) | (mm) | (mm) | (%) |
| 4 | 4,000 | 25.96 | 5.45 | 19.99 | 0.50 |
| 3 | 4,000 | 20.52 | 6.38 | 23.42 | 0.59 |
| 2 | 4,000 | 14.12 | 8.07 | 29.61 | 0.74 |
| 1 | 4,250 | 6.05 | 6.05 | 22.19 | 0.52 |
| Base | 0 | - | - | - | - |

**Table 9.** Story drift fixed-base structure in y-direction

| Story | Floor Height h | Displ $\delta_Y$ | Elastic Drift $\Delta_{elastic}$ | Inelastic Drift $\Delta_{inelastic}$ | Drift Ratio Y |
|---|---|---|---|---|---|
| | (mm) | (mm) | (mm) | (mm) | (%) |
| 4 | 4,000 | 33.30 | 5.42 | 19.87 | 0.50 |
| 3 | 4,000 | 27.88 | 10.65 | 39.05 | 0.98 |
| 2 | 4,000 | 17.23 | 9.97 | 36.54 | 0.91 |
| 1 | 4,250 | 7.27 | 7.27 | 26.65 | 0.63 |
| Base | 0 | - | - | - | - |

**Table 10.** Story drift SSI structure in x-direction

| Story | Floor Height h | Displ. $\delta_X$ | Total Drift $\Delta_{total}$ | Rotation $\theta$ | Displ. Rotation $\delta_\theta$ | Horizontal Drift $\Delta^*$ | Elastic Drift $\Delta_{elastic}$ | Inelastic Drift $\Delta_{inelastic}$ | Drift Ratio X |
|---|---|---|---|---|---|---|---|---|---|
| | (mm) | (mm) | (mm) | (rad) | (mm) | (mm) | (mm) | (mm) | (%) |
| 4 | 4,000 | 29.85 | 4.646 | 0.000917 | 3.668 | 0.978 | 0.978 | 3.586 | 0.09 |
| 3 | 4,000 | 25.21 | 6.311 | 0.000917 | 3.668 | 2.643 | 2.643 | 9.691 | 0.24 |
| 2 | 4,000 | 18.89 | 8.317 | 0.000917 | 3.668 | 4.649 | 4.649 | 17.046 | 0.43 |
| 1 | 4,250 | 10.58 | 8.584 | 0.000917 | 3.897 | 4.687 | 4.687 | 17.185 | 0.40 |
| Base | 0.0 | 1.99 | 1.993 | 0.000000 | 0.000 | 1.993 | 1.993 | 7.308 | 0.05 |

**Table 11.** Story drift SSI structure (SSI) y-direction

| Story | Floor Height h | Displ. $\delta_Y$ | Total Drift $\Delta_{total}$ | Rotation $\theta$ | Displ. Rotation $\delta_\theta$ | Horizontal Drift $\Delta^*$ | Elastic Drift $\Delta_{elastic}$ | Inelastic Drift $\Delta_{inelastic}$ | Drift Ratio Y |
|---|---|---|---|---|---|---|---|---|---|
| | (mm) | (mm) | (mm) | (rad) | (mm) | (mm) | (mm) | (mm) | (%) |
| 4 | 4,000 | 37.37 | 5.410 | 0.000812 | 3.248 | 2.162 | 2.162 | 7.927 | 0.20 |
| 3 | 4,000 | 31.96 | 9.751 | 0.000812 | 3.248 | 6.503 | 6.503 | 23.844 | 0.60 |
| 2 | 4,000 | 22.21 | 10.109 | 0.000812 | 3.248 | 6.861 | 6.861 | 25.157 | 0.63 |
| 1 | 4,250 | 12.11 | 9.933 | 0.000812 | 3.451 | 6.482 | 6.482 | 23.767 | 0.56 |
| Base | 0.0 | 2.16 | 2.168 | 0.000812 | 0.000 | 2.168 | 2.168 | 7.949 | 0.05 |

 https://doi.org/10.1051/e3sconf/202560413003

The story drift comparison results are also presented in Figs. 11 and 12 below.

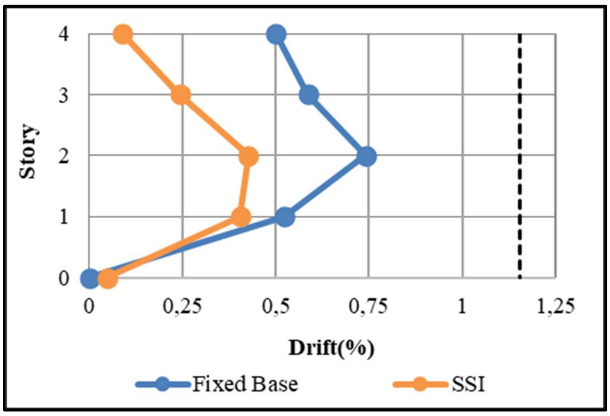


**Fig 11.** Story drift in x-direction

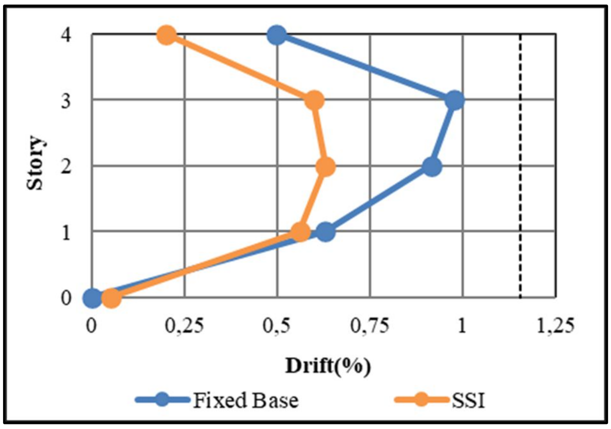


**Fig 12.** Story drift in y-direction

### 4.4 Capacity curve and performance points

The results of the comparison of the two structural models show that the consideration of SSI in the existing structure resulted in an increase in the performance point value. The comparison of the capacity curves of the two models in the X and Y directions is presented in Figs. 13 and 14.

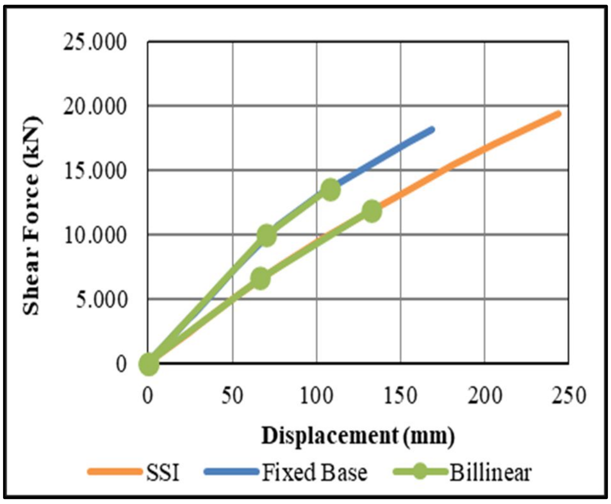


**Fig 13.** Capacity curves in x-direction

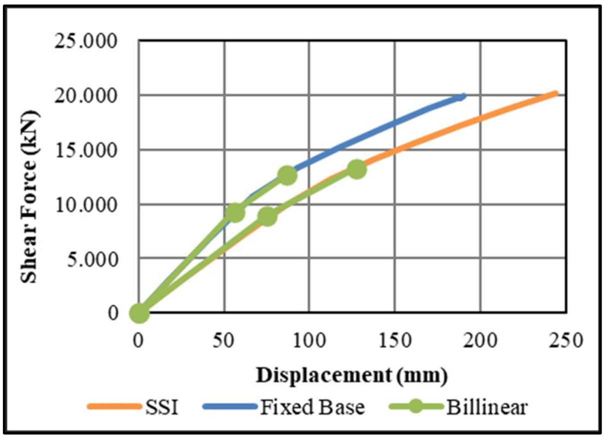


**Fig 14.** Capacity curves in y-direction

The performance points generated from the capacity curves for model 1 (fixed base) and model 2 (SSI) in the X and Y directions are shown in Table 12 as follows.

**Table 12.** Performance point

| Model | Directions | Displacement (mm) | Shear Force (kN) |
|---|---|---|---|
| Model 1 (Fixed Base) | X | 107.9 | 13,613.8 |
| | Y | 86.4 | 12,667.2 |
| Model 2 (SSI) | X | 132.7 | 11,906.1 |
| | Y | 127.2 | 13,297.5 |

From the table above, it can be seen that the displacement that occurs in the SSI model is greater than the fixed-base model at the performance point.

### 4.5 Plastic joint mechanism

The results of the comparison of the two structural models shows that the presence of SSI considerations in the existing structure results in changes in the plastic joint mechanism. The plastic hinge mechanisms produced through nonlinear pushover analysis on each structural model are presented in Figs. 15 to 18 below.

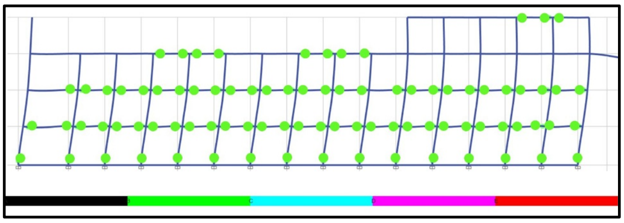

**Fig 15.** Plastic hinge mechanism of fixed base structure in x-direction

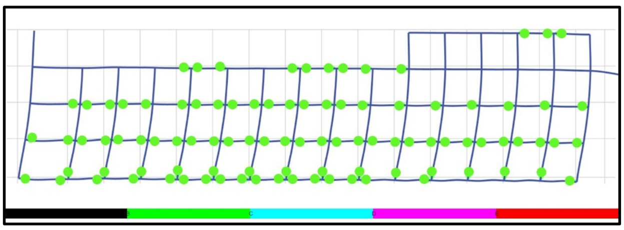

**Fig 16.** Plastic hinge mechanism of SSI structure in x-direction

From Figs. 15-18, there is no significant difference in the plastic joints that occur in either the fixed-base model or the SSI model. In the SSI model, there is plastification in the tie-beams at the base of the column because the base joint can be displaced.

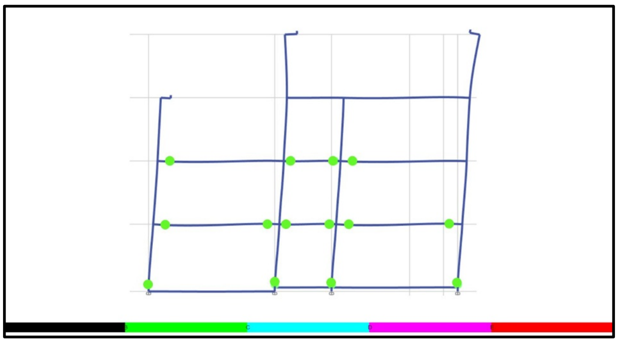

**Fig 17.** Plastic hinge mechanism fixed base structure in y-direction

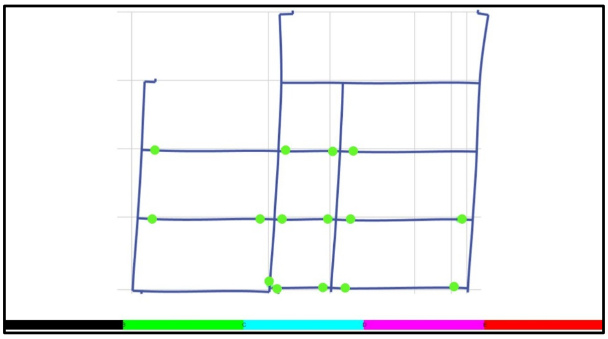

**Fig 18.** Plastic hinge mechanism SSI structure in y-direction

## 5 Conclusions

The effect of soil-structure interaction on a 4-story building located in Pekanbaru has been analyzed in this study. The conclusions obtained from this research are:

1. There is an increase in the natural period of the structure when SSI is considered. The increase in the SSI model is 20% in the X direction and 18% in the Y direction.
2. There is a decrease in the base shear force when SSI is considered by 18% in the X direction and 16% in the Y direction.
3. There is an increase in the maximum displacement of each floor when SSI is considered. With an average percentage of 29% in the X direction and 24% in the Y direction.
4. Nonlinear pushover analysis results in an increase in the performance point value of the structure with SSI modeling. The tie-beam at the base of the structure has plastification because the base joint can be displaced.

## References

1 F. M. Wani, J. Vemuri, C. Rajaram, D. V. Babu R, Effect of soil structure interaction on the dynamic response of reinforced concrete structures. Nat. Hazards Res., **2** (2022). https://doi.org/10.1016/j.nhres.2022.11.002.

2 S. Mokhles Al Samadi, Resonance effect on structures subjected to earthquake loads due to soil structure interaction (University of Jordan, Amman, 2014). https://doi.org/10.13140/RG.2.1.2380.1760.

3 A. Yanik, Y. Ulus, Soil–structure interaction consideration for base isolated structures under earthquake excitation. Buildings. **13** (2023). https://doi.org/10.3390/buildings13040915.

4 A. Kurniawandy, S. Nakazawa, A proposal of seismic index for existing buildings in Indonesia using pushover analysis. J. Eng. Technol. Sci., **52** (2020). https://doi.org/10.5614/j.eng.technol.sci.2020.52.3.2.

5 S. B. Magade, R. K. Ingle, Influence of clear edge distance and spacing of piles on failure of pile cap. Iran. J. Sci. Technol. - Trans. Civ. Eng., **44** (2020). https://doi.org/10.1007/s40996-019-00285-9.

6 A. Kurniawandy, S. Nakazawa, Seismic performance evaluation of existing building using seismic index method. MATEC Web Conf., **276** (2019). https://doi.org/10.1051/matecconf/201927601015.

7 A. Kurniawandy, S. Nakazawa, A. Hendry, Ridwan, R. Firdaus, Structural building screening and evaluation International Conference in Civil Engineering 2017. AIP Conf. Proc. 020031 (2017)

8 Indonesian code, *SNI 1726:2019* earthquake resistant design code for building and non-building of Indonesia (in Indonesian) (Standardization Agency of Indonesia, Jakarta, 2019)

9 American Society of Civil Engineers., ASCE/SEI 41-13 seismic evaluation and retrofit of existing building. (Reston, Virginia, 2013)